A Numerical Solution of Unsteady Flow in a Two-Dimensional Square Cavity

LEO F. DONOVAN*
NASA Lewis Research Center, Cleveland, Ohio

The continuity equation and unsteady Navier-Stokes equations are solved numerically for two-dimensional flow in a square cavity. The fluid is initially at rest and the upper surface of the cavity moves with constant velocity throughout the calculation. Good agreement is shown between the calculated position of the vortex center at large times and the position of an experimentally determined vortex center. Velocity profiles at large times are in excellent agreement with those calculated from an extant solution of the steady Navier-Stokes equations. The unsteady results are also recorded as a computer-generated motion picture of "marked particles" that move with the fluid and serve to make the flow visible. A sequence of photographs from the movie is presented.

Nomenclature†

d = discrepancy term in continuity equation
i,j = subscripts denoting grid indices
L = reference length
n = superscript denoting nth time step
q = subscript denoting qth iteration
Re = Reynolds number $LU\bar{\nu}$
r = abbreviation, Eq. (7)
t = time, $\bar{t}U/L$
U = reference velocity
u = velocity in x direction, $\bar{u}/U$
v = velocity in y direction, $\bar{v}/U$
x = horizontal direction, $\bar{x}/L$
y = vertical direction, $\bar{y}/L$
δt = time step
$\delta x, \delta y$ = space increments
$\bar{\nu}$ = kinematic viscosity of fluid
$\bar{\rho}$ = density of fluid
ϕ = pressure, $\bar{p}/\bar{\rho}U^2$

Introduction

THE availability of large, high-speed computers allows one to attack some formidable and interesting problems. One area of research open to investigation is in the solution of nonlinear partial differential equations describing physical phenomena. Analytic solutions can only be obtained for certain special cases and, in addition, the nonlinearity of the equations makes them much more difficult to solve numerically than linear equations, for which numerical techniques have been developed. However, some progress has been made. The recent book by Ames[1] summarizes much of this work.

An additional difficulty with numerical solutions of partial differential equations is that they provide a mass of detailed information that is very hard to assimilate and understand. The most imaginative solution to this problem is due to Fromm and Harlow[2] who have devised a visual display technique for presenting the results of their fluid dynamics calculations. This technique is analogous to a flow visualization experiment in the laboratory, in which a tracer is introduced into a fluid to make the flow visible.

Fluid motion is governed by the continuity equation and Navier-Stokes equations, expressing conservation of mass and momentum. Almost all the numerical solutions of these equations have been for two-dimensional flows. Some investigators have transformed the equations to stream function and vorticity coordinates. Pearson,[3] for example, has treated rotating disks in this manner. Other investigators have chosen to retain velocity and position coordinates. Work by Harlow et al.[4] on free surface flows falls in this category. The latter techniques appear easier to extend to three-dimensional flows.

As the first step in a program to solve the equations describing unsteady flows we have chosen to investigate constant density, two-dimensional flow in a square cavity. This problem has relevance in bearing and seal studies, is difficult to study experimentally without disturbing the flow, and is interesting in its own right. Cavity flow has been investigated experimentally and numerically so that comparison with prior work is possible. In addition, since no fluid enters or leaves the cavity, the boundary conditions that must be satisfied by the equations are easily handled. Since Harlow's method[4] has the advantages of combining a successful numerical technique with visual display, we have adopted it and modified it to our needs.

If the upper surface of a cavity filled with fluid is moving in its own plane with constant velocity, a circulatory motion of the fluid is set up within the cavity. This is illustrated schematically in Fig. 1. Time exposure photographs have been taken[5,6] of flows into which a tracer has been injected so that the qualitative features of the steady flow are known. Most of the fluid rotates about a point, called the vortex center, where the vector velocity is zero. In a square cavity the main vortex occupies most of the cavity and small counter-rotating vortices exist in both lower corners.

Steady flow in a two-dimensional cavity has been analyzed[5,7–9] by numerically integrating the steady Navier-Stokes equations. Burggraf[7] has also obtained an analytic solution to the linearized problem for an eddy bounded by a circular streamline. The starting flow problem, the fluid

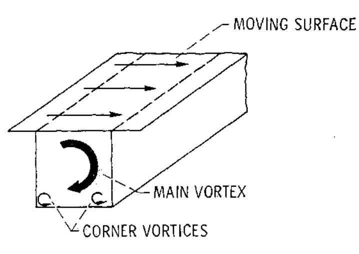

Fig. 1 Schematic diagram of cavity.

Received March 3, 1969; revision received August 4, 1969.
* Aerospace Engineer, Fundamental Heat Transfer Branch.
† Dimensional quantities are denoted by an overbar.

being initially at rest, was considered by Greenspan[10]; however, only steady results were presented.

This paper describes a numerical technique for the solution of the unsteady Navier-Stokes equations. As an illustration of the technique, the problem of unsteady flow in a square cavity at a Reynolds number of 100, based on the length and velocity of the moving surface and the viscosity of the fluid, is solved. Velocity profiles from the unsteady solution at large times are compared with velocity profiles from extent solutions of the steady equations and good agreement is found. The calculated position of the vortex center at large times is found to be the same as an experimentally determined steady vortex center. In addition, the results of the calculations are illustrated by showing the development of the flow, starting from rest, in a sequence of photographs from a movie in which "marked particles" are used to make the flow visible.

Analysis

Differential Equations

The dimensionless forms of the constant density, two-dimensional continuity equation and Navier-Stokes equations for a Newtonian fluid can be written as[4]

$$\partial u/\partial x + \partial v/\partial y = 0 \tag{1}$$

$$\frac{\partial u}{\partial t} + \frac{\partial u^2}{\partial x} + \frac{\partial uv}{\partial y} = -\frac{\partial \phi}{\partial x} + Re^{-1}\left[\frac{\partial^2 u}{\partial y^2} - \frac{\partial^2 v}{\partial x \partial y}\right] \tag{2}$$

$$\frac{\partial v}{\partial t} + \frac{\partial v^2}{\partial y} + \frac{\partial uv}{\partial x} = -\frac{\partial \phi}{\partial y} + Re^{-1}\left[\frac{\partial^2 v}{\partial x^2} - \frac{\partial^2 u}{\partial x\, \partial y}\right] \tag{3}$$

For the cavity flow problem it is convenient to choose the length and velocity of the moving wall as the reference length and velocity.

If the x and y momentum equations are differentiated with respect to x and y, and the results added, one obtains

$$\frac{\partial^2 \phi}{\partial x^2} + \frac{\partial^2 \phi}{\partial y^2} = -\frac{\partial}{\partial t}\left(\frac{\partial u}{\partial x} + \frac{\partial v}{\partial y}\right) - \frac{\partial^2 u^2}{\partial x^2} - 2\frac{\partial^2 uv}{\partial x \partial y} - \frac{\partial^2 v^2}{\partial y^2} \tag{4}$$

The finite difference form of this Poisson's equation, with source term a function of the velocities, is solved iteratively at each time step using successive over-relaxation. With pressures known, the finite difference forms of Eqs. (2) and (3) are solved explicitly for velocities. The reason for retaining the first term on the right of the equality sign will be discussed when the difference equations are derived.

Since the fluid is at rest in the cavity at the start of the calculation, the initial condition is that the velocities are everywhere zero. The boundary conditions require the normal and tangential velocities to vanish at the walls, except at the moving wall where the tangential component of velocity attains the constant wall velocity. A reference pressure of unity is chosen at the center of the wall opposite the moving wall.

Difference Equations

The positions of the variables on the finite difference mesh are shown in Fig. 2. Note that each velocity component and the pressure are defined at different cell positions. If centered differences are used, Eq. (1) can be written

$$d_{i,j} = (1/\delta x)(u_{i,j+\frac{1}{2}} - u_{i,j-\frac{1}{2}}) + (1/\delta y)(v_{i+\frac{1}{2},j} - v_{i-\frac{1}{2},j}) \tag{5}$$

In order to satisfy the continuity equation it is necessary that $d = 0$. However, the finite difference form of Eq. (4) for the pressure is not solved exactly so that in general, after calculating the velocities, there will be a nonzero value of d at each mesh point. In order to compensate for this, the term that involves this discrepancy from the previous time

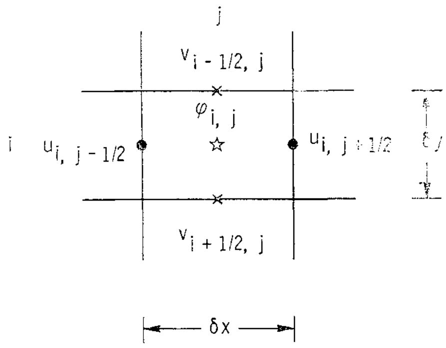

Fig. 2 Position of variables on finite-difference mesh.

is retained in the finite difference form of the pressure equation for the present time (this is discussed in Ref. 11).

If Eq. (4) is written in finite difference form, the equation for the pressure is

$$\phi_{i,j} = \frac{1}{2(1/\delta x^2 + 1/\delta y^2)}\left(\frac{\phi_{i,j+1} + \phi_{i,j-1}}{\delta x^2} + \frac{\phi_{i+1,j} + \phi_{i-1,j}}{\delta y^2} + r_{i,j}\right) \tag{6}$$

where

$$r_{i,j} = (1/\delta x^2)(u^2_{i,j+1} - 2u^2_{i,j} + u^2_{i,j-1}) + (2/\delta x\delta y)[(uv)_{i+\frac{1}{2},j+\frac{1}{2}} - (uv)_{i-\frac{1}{2},j+\frac{1}{2}} - (uv)_{i+\frac{1}{2},j-\frac{1}{2}} + (uv)_{i-\frac{1}{2},j-\frac{1}{2}}] + (1/\delta y^2)(v^2_{i+1,j} - 2v^2_{i,j} + v^2_{i-1,j}) - (1/\delta t)d_{i,j} \tag{7}$$

The finite difference forms of Eqs. (2) and (3) become

$$u^{n+1}_{i,j+\frac{1}{2}} = u_{i,j+\frac{1}{2}} + \delta t\{-(1/\delta x)(u^2_{i,j+1} - u^2_{i,j}) - (1/\delta y)[(uv)_{i+\frac{1}{2},j+\frac{1}{2}} - (uv)_{i-\frac{1}{2},j+\frac{1}{2}}] - (1/\delta x)(\phi_{i,j+1} - \phi_{i,j}) + Re^{-1}[(1/\delta y^2)(u_{i+1,j+\frac{1}{2}} - 2u_{i,j+\frac{1}{2}} + u_{i-1,j+\frac{1}{2}}) - (1/\delta x\delta y)(v_{i+\frac{1}{2},j+1} - v_{i+\frac{1}{2},j} - v_{i-\frac{1}{2},j+1} + v_{i-\frac{1}{2},j})]\} \tag{8}$$

$$v^{n+1}_{i+\frac{1}{2},j} = v_{i+\frac{1}{2},j} + \delta t\{-(1/\delta x) \times [(uv)_{i+\frac{1}{2},j+\frac{1}{2}} - (uv)_{i+\frac{1}{2},j-\frac{1}{2}}] - (1/\delta y)(v^2_{i+1,j} - v^2_{i,j}) - (1/\delta y)(\phi_{i+1,j} - \phi_{i,j}) + Re^{-1}[(1/\delta x^2)(v_{i+\frac{1}{2},j+1} - 2v_{i+\frac{1}{2},j} + v_{i+\frac{1}{2},j-1}) - (1/\delta x\delta y)(u_{i+1,j+\frac{1}{2}} - u_{i,j+\frac{1}{2}} - u_{i+1,j-\frac{1}{2}} + u_{i,j-\frac{1}{2}})]\} \tag{9}$$

The superscript $n + 1$ refers to the future time [$t = (n + 1)\delta t$]; terms without superscripts are known from the present time ($t = n\delta t$).

Because of the way in which the variables are defined on the finite difference mesh, the cavity walls pass through cell positions where the normal components of velocity are defined. Thus, boundary conditions involving the normal component of velocity are specified directly. Values of the tangential components of velocity that fall outside the cavity are chosen so that the interpolated values at the wall satisfy the boundary conditions. For example, if the left boundary is a stationary wall at $j + \frac{1}{2}$,

$$u_{i,j+\frac{1}{2}} = 0 \tag{10}$$

and

$$v_{i+\frac{1}{2},j} = -v_{i+\frac{1}{2},j+1} \tag{11}$$

Values of ϕ outside the cavity that are required in the solution of the finite difference Poisson's equation for pressure can be obtained from the appropriate momentum equation.

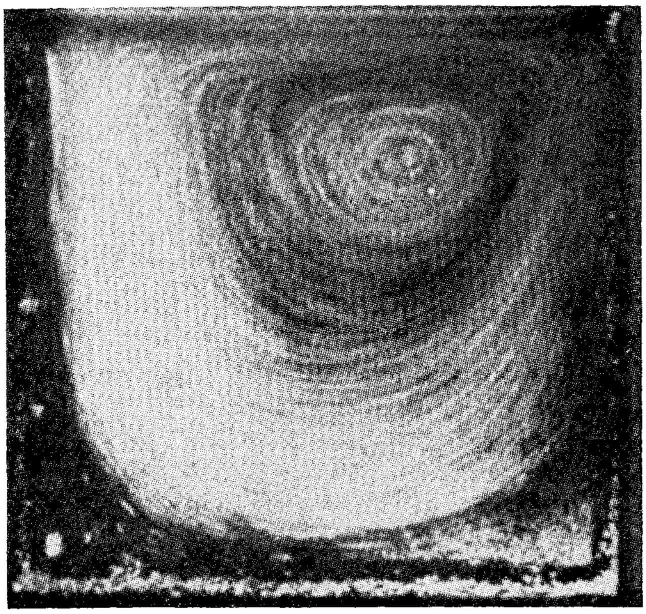

Fig. 3 Photograph of experimental vortex.[5]

For example, if the left boundary at $j + \frac{1}{2}$ is a stationary wall,

$$u^{n+1}{}_{i,j+\frac{1}{2}} = u^{n}{}_{i,j+\frac{1}{2}} = 0 \quad (12)$$

so that

$$\phi_{i,j} = \phi_{i,j+1} + 2(Re^{-1}/\delta y)(v_{i+\frac{1}{2},j+1} - v_{i-\frac{1}{2},j+1}) \quad (13)$$

When carrying out the finite differencing, averages are used for quantities that are not defined, e.g.,

$$u_{i,j} = \tfrac{1}{2}(u_{i,j+\frac{1}{2}} + u_{i,j-\frac{1}{2}}) \quad (14)$$

When the derivative of a product of such quantities is formed, the product is differentiated and then averages are formed, e.g.,

$$\partial^2(uv)_{i,j}/\partial x\, \partial y = (1/\delta x\, \delta y)[(uv)_{i+\frac{1}{2},j+\frac{1}{2}} - (uv)_{i-\frac{1}{2},j+\frac{1}{2}} - (uv)_{i+\frac{1}{2},j-\frac{1}{2}} + (uv)_{i-\frac{1}{2},j-\frac{1}{2}}] \quad (15)$$

and then, e.g.,

$$(uv)_{i+\frac{1}{2},j+\frac{1}{2}} = \tfrac{1}{4}(u_{i+1,j+\frac{1}{2}} + u_{i,j+\frac{1}{2}})(v_{i+\frac{1}{2},j+1} + v_{i+\frac{1}{2},j}) \quad (16)$$

Since the new velocities are calculated explicitly, the time step is limited by stability conditions. Hirt[12] has suggested approximate criteria

$$Re^{-1} > \tfrac{1}{2}\delta t u^2 \quad (17)$$

and

$$Re^{-1} > \tfrac{1}{2}\delta x^2 \partial u/\partial x \quad (18)$$

where u is the average maximum fluid speed and $\partial u/\partial x$ is the average maximum velocity gradient in the direction of flow.

The finite difference equations were coded in FORTRAN IV. Additional coding was required for auxiliary calculations, particle movements, plotting routines, etc. At each time step the magnitudes of d were checked to insure that they were less than 3.5×10^{-3}.[4] The convergence criterion used for the pressure iteration was[4]

$$|\phi_q - \phi_{q-1}|/(|\phi_q| + |\phi_{q-1}| + u^2{}_{i,j} + v^2{}_{i,j}) < 2 \times 10^{-4} \quad (19)$$

where the subscript q indicates the qth iteration.

A Reynolds number of 100 was selected for the illustrative calculation because a photograph of a steady experimental vortex and results of the solution of the steady Navier-Stokes equations are available for comparison. The first stability criterion suggests a time step of 0.02. Equal space increments of 0.05 were used and it was observed that the second criterion was satisfied also. No evidence of instability was noted during the course of the calculation. About 8 min are required on the IBM 360/67 to carry out the calculations to a dimensionless time of 10. An additional 4 min are necessary to produce the microfilm output.

The calculations were also performed with space and time increments halved and essentially the same results were obtained. Runs with larger time increments and runs at higher Reynolds numbers indicate that, for this cavity flow, the stability criteria are somewhat conservative. However, if the microfilmed motion of the marked particles is to be made into a movie, the smaller time increments are desirable.

Marked Particles

At the start of the calculation the marked particles are assumed to be distributed throughout the fluid in some known manner. We have used a uniform distribution of four particles per cell. The marked particles are moved with the fluid and photographed at each time step during the course of the calculation. The marked particles serve to make the flow visible so that the sequence of photographs, when viewed as a motion picture, shows the behavior of the fluid clearly. The use of marked particles to display the results of solutions of the Navier-Stokes equations is not to be confused with other ways of showing the results, such as streamlines, streak lines, or path lines. It should be noted that the marked particles do not enter into the solution of the Navier-Stokes equations.

The velocity components for each particle were initially calculated as a weighted average of the velocities at the four nearest mesh points. Thus, for particles within half a mesh spacing of a wall, two of the mesh points used for calculating the tangential component of velocity lay outside the cavity. Some difficulty was encountered with particle movement near the wall where the boundary layer was very thin. It was noticed that particles tended to congregate along the extreme upper part of the right wall. Then a crescent shaped region devoid of particles formed along most of the remaining part of the right wall and extended into the cavity. In order to circumvent this problem the calculation of tangential velocity components of particles within half a mesh spacing of a wall was modified to use only velocities at the two mesh points inside the cavity. This resulted in a tangential velocity component that did not vary in a direction normal to the wall in the half mesh closest to the wall. Thereafter no anomalous particle motion was noted and this problem was not pursued further.

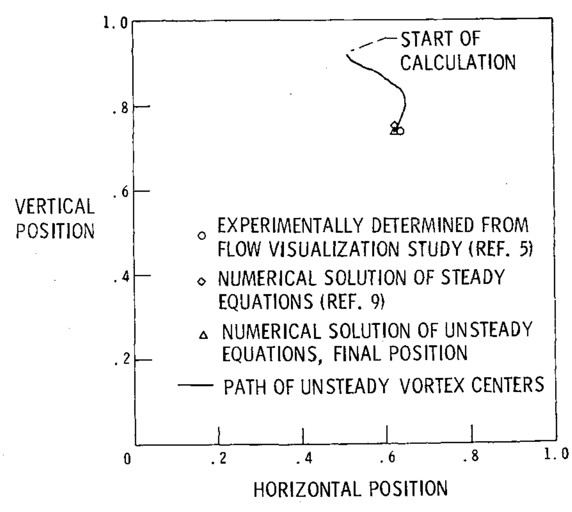

Fig. 4 Position of vortex center.

Discussion of Results

The results of the calculation will be presented in two parts, viz., 1) numerical comparisons with experiment and prior calculation, and 2) a visual display of the development of the flow. For cavity flow numerical comparisons are possible only at steady conditions; unsteady results, such as the visual display, are new. The computer and a microfilm plotter were used to produce all the plots of data as well as the motion picture.

Numerical

The position of the experimental vortex center can be determined from flow visualization studies. Figure 3 shows a time exposure photograph of steady flow in a square cavity at a Reynolds number of about 100.[5] Washing powder has been added to oil to make the flow visible. A tape is pulled across the cavity to provide the moving surface. The position of the vortex center was obtained from an enlargement of Fig. 3.

The position of this experimental vortex center and the position of a vortex center calculated from a solution of the steady Navier-Stokes equation (9) are compared in Fig. 4 with the position of the vortex center at large times calculated from the solution of the unsteady Navier-Stokes equations. These three are in good agreement.

Since the position of the vortex center changes during the solution of the unsteady equation, its instantaneous position is of interest and was determined during the course of the calculation. Also shown in Fig. 4 is the instantaneous position of the vortex center. It moves, rapidly at first and then more slowly, from a position under the midpoint of the moving surface to its terminal position.

Figures 5 and 6 compare velocity traverses through the vortex center calculated from the steady[9] and unsteady Navier-Stokes equations at large times. Figure 5 is a traverse perpendicular to the moving surface and plots vertical position vs velocity component parallel to the moving surface. Figure 6 is a traverse parallel to the moving surface and shows velocity component perpendicular to the moving surface vs horizontal position. The excellent agreement indicates that the unsteady solution is numerically correct for large times. Further confimation of the steady result shown in Fig. 5 is provided by Ref. 7, in which a numerical solution of the steady Navier-Stokes equations gave essentially the same results as Ref. 9.

A way of illustrating the pressure distribution is shown by the three-dimensional view in Fig. 7. The large pressure

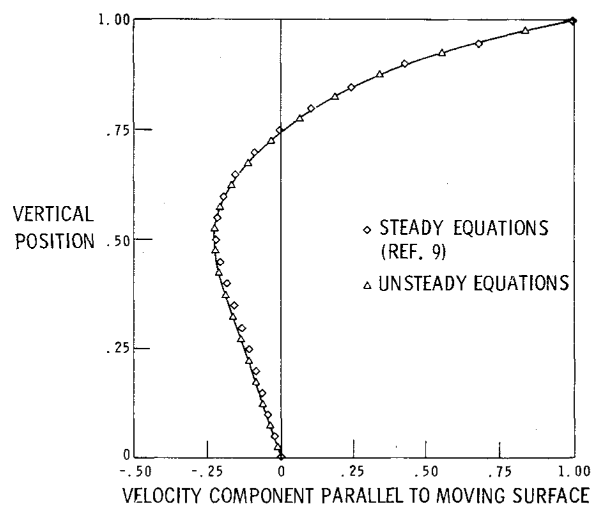

Fig. 5 Velocity traverse in vertical direction through vortex center.

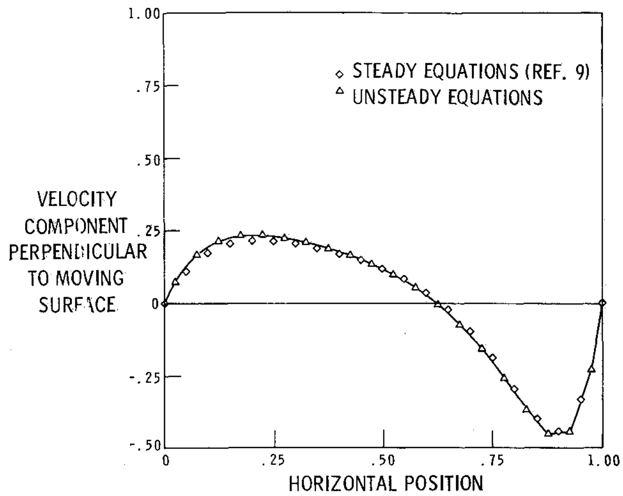

Fig. 6 Velocity traverse in horizontal direction through vortex center.

maximum at the stagnation point is evident; the shallow pressure minimum at the vortex center is less distinct. Another method of displaying pressures is by a contour plot (e.g., Ref. 7). These two ways of presenting the same data, one qualitative and the other quantitative, complement each other. The pressure at the vortex center shown in Fig. 7 agrees with the pressure obtained in Ref. 7.

Visual

The sequence of photographs of instantaneous particle positions made by the microfilm recorder constitutes a motion picture. Enlargements of several frames are shown in Fig. 8. The small triangle above the cavity is used to show the velocity of the moving surface. Figure 8a shows the initial uniform distribution of particles within the cavity. The remaining figures show that the fluid close to the upper moving surface is dragged along by the upper surface and forced to turn down at the right wall. The fluid flows along the right wall, gradually turning back to the left and then upward, only to be directly influenced by the moving surface and dragged to the right again. This flow pattern is clearly seen in the movie.

The lower corners remain relatively quiescent and some order is evident even on the last frame. Examination of the velocities at the mesh point shows the beginning of the counterrotating vortices in the lower corners. The calculations have not been carried to large enough times for them to be visible in the movie. (Copies of the film are available for loan on request to the author.)

Concluding Remarks

Unsteady flow in a square cavity has been analyzed by solving numerically the Navier-Stokes equations. The fluid

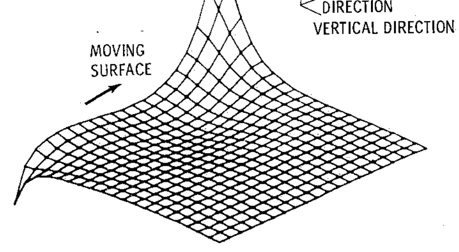

Fig. 7 Pressure distribution.

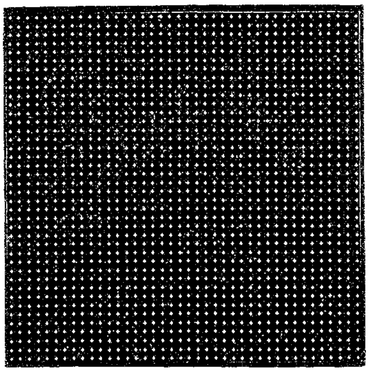

Fig. 8a Time = 0

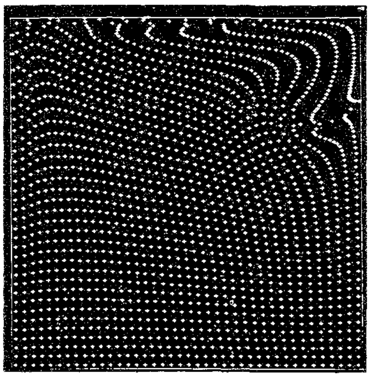

Fig. 8b Time = 1

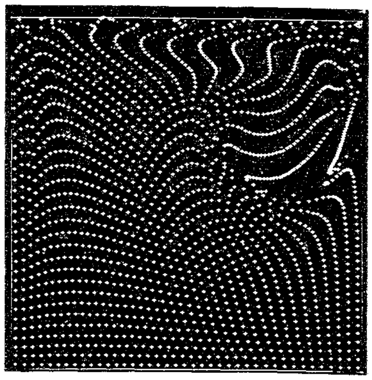

Fig. 8c Time = 2

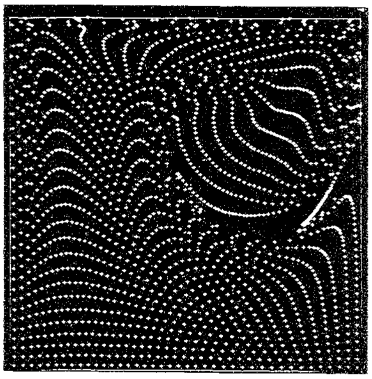

Fig. 8d Time = 3

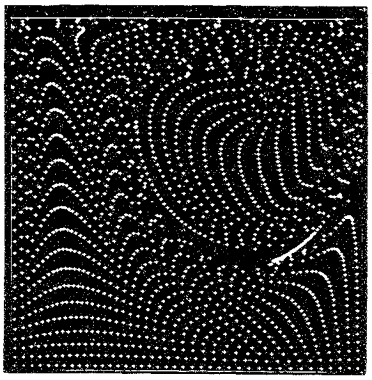

Fig. 8e Time = 4

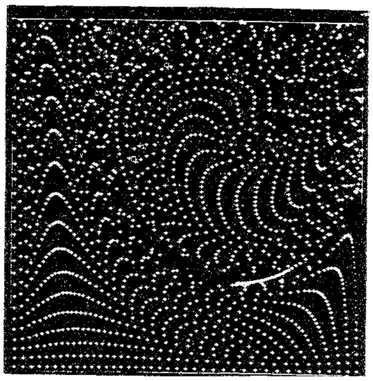

Fig. 8f Time = 5

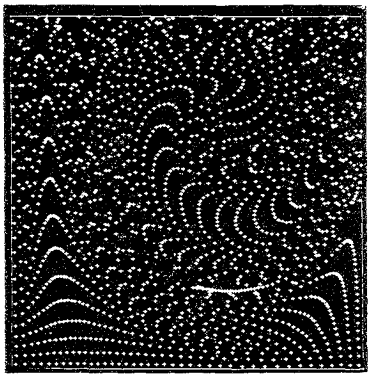

Fig. 8g Time = 6

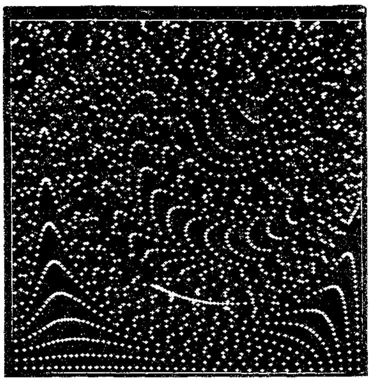

Fig. 8h Time = 7

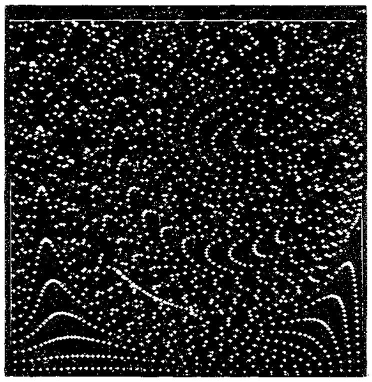

Fig. 8i Time = 8

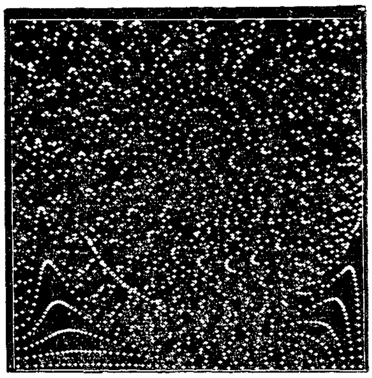

Fig. 8j Time = 9

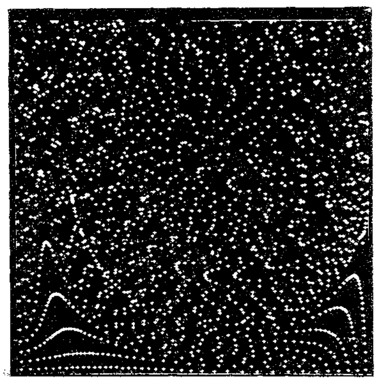

Fig. 8k Time = 10

Fig. 8 Enlargement of frames of movie.

is initially at rest and the upper surface moves in its own plane with constant velocity. For the illustrative calculation the Reynolds number, based on the length and velocity of the moving surface and the viscosity of the fluid, was chosen as 100 so that a comparison could be made with an experiment as well as with extant solutions of the steady Navier-Stokes equations.

1) The terminal position of the calculated vortex center is in agreement with an experimentally determined steady vortex center.

2) Velocity and pressure distributions at large times agree with previous solutions of the steady Navier-Stokes equations, indicating that the unsteady solution gives the correct steady results.

3) "Marked particles" were used to show the development of the flow from rest. This method of displaying computed results simulates a flow visualization study in the laboratory and shows clearly the behavior of the fluid.

References

[1] Ames, W. F., *Nonlinear Partial Differential Equations in Engineering*, Academic Press, New York, 1965.

[2] Fromm, J. E. and Harlow, F. H., "Numerical Solution of the Problem of Vortex Street Development," *The Physics of Fluids*, Vol. 6, No. 7, July 1963, pp. 975–982.

[3] Pearson, C. E., "Numerical Solutions for the Time-Dependent Viscous Flow Between Two Rotating Coaxial Disks," *Journal of Fluid Mechanics*, Vol. 21, Pt. 4, April 1965, pp. 623–633.

[4] Welch, J. E. et al., "The MAC Method—A Computing Technique for Solving Viscous, Incompressible, Transient Fluid-Flow Problems Involving Free Surfaces," LA-3425, March 21, 1966, Los Alamos Scientific Lab., Los Alamos, N. Mex.; see also Harlow, F. H. and Welch, J. E., "Numerical Calculation of Time-Dependent Viscous Incompressible Flow of Fluid with Free Surface," *The Physics of Fluids*, Vol. 8, No. 12, Dec. 1965, pp. 2182–2189; Harlow, F. H. and Welch, J. E., "Numerical Study of Large-Amplitude Free-Surface Motions," *The Physics of Fluids*, Vol. 9, No. 5, May 1966, pp. 842–851; Daly, B. J., "Numerical Study of Two Fluid Rayleigh-Taylor Instability," *The Physics of Fluids*, Vol. 10, No. 2, Feb. 1967, pp. 297–307.

[5] Mills, R. D., "Numerical Solutions of the Viscous Flow Equations for a Class of Closed Flows," *Journal of the Royal Aeronautical Society*, Vol. 69, No. 658, Oct. 1965, pp. 714–718.

[6] Pan, F. and Acrivos, A., "Steady Flows in Rectangular Cavities," *Journal of Fluid Mechanics*, Vol. 28, Pt. 4, June 22, 1967, pp. 643–655.

[7] Burggraf, O. R., "Analytical and Numerical Studies of the Structure of Steady Separated Flows," *Journal of Fluid Mechanics*, Vol. 24, Pt. 1, Jan. 1966, pp. 113–151.

[8] Runchal, A. K., Spalding, D. B., and Wolfshtein, M., "The Numerical Solution of the Elliptic Equations for Transport of Vorticity, Heat and Matter in Two-Dimensional Flows," SF/TN/2, Aug. 1967, Imperial College of Science and Technology, London, England.

[9] Zuk, J. and Renkel, H. E., "Numerical Solutions for the Flow and Pressure Fields in an Idealized Spiral Grooved Pumping Seal," Paper FICFS-30, presented at the Fourth International Conference on Fluid Sealing, May 8, 1969, Philadelphia, Pa.

[10] Greenspan, D. et al., "Work in Progress at the Mathematics Research Center on the Numerical Solution of the Navier-Stokes Equations," *Proceedings of the ARO Working Group on Computers*, Rept. AROD-65-1, DDC AD-613592, Feb. 1965, Army Research Office, Durham, N. C., pp. 213–260.

[11] Hirt, C. W. and Harlow, F. H., "A General Corrective Procedure for the Numerical Solution of Initial Value Problems," *Journal of Computational Physics*, Vol. 2, No. 2, Nov. 1968, pp. 114–119.

[12] Hirt, C. W., "Heuristic Stability Theory for Finite-Difference Equations," *Journal of Computational Physics*, Vol. 2, No. 4, June 1968, pp. 339–355.